Energy conversion in Textus Bioactiv Ag membrane dressings using Peusner's network thermodynamic descriptions

Konwersja energii w opatrunku membranowym Textus Bioactive Ag w opisie termodynamiki sieciowej Peusnera

Kornelia M. Batko[1,B,C], Izabella Ślęzak-Prochazka[2,B,C], Sławomir Marek Grzegorczyn[3,A,D–F], Anna Pilis[4,B], Paweł Dolibog[3,B], Andrzej Ślęzak[4,A,D–F]

[1] Faculty of Social Sciences, University of Silesia, Katowice, Poland
[2] Biotechnology Centre, Silesian University of Technology, Gliwice, Poland
[3] Department of Biophysics, Faculty of Medical Sciences in Zabrze, Medical University of Silesia, Poland
[4] Department of Health Science and Physiotherapy, Jan Dlugosz University, Częstochowa, Poland

A – research concept and design; B – collection and/or assembly of data; C – data analysis and interpretation; D – writing the article; E – critical revision of the article; F – final approval of the article

Polymers in Medicine, ISSN 0370-0747 (print), ISSN 2451-2699 (online) *Polim Med*. 2022;52(2):57–66

Address for correspondence
Sławomir Marek Grzegorczyn
E-mail: grzegorczyn@sum.edu.pl

Funding sources
This work was supported by the project of Medical University of Silesia No. PCN-1-172/N/0/I.

Conflict of interest
None declared

Received on May 18, 2022
Reviewed on June 13, 2022
Accepted on September 5, 2022

Published online on November 10, 2022

Cite as
Batko KM, Ślęzak-Prochazka I, Grzegorczyn SM, Pilis A, Dolibog P, Ślęzak A. Energy conversion in Textus Bioactiv Ag membrane dressings using Peusner's network thermodynamic descriptions. *Polim Med*. 2022;52(2):57–66. doi:10.17219/pim/153522

DOI
10.17219/pim/153522

Abstract

Background. The Textus Bioactiv Ag membrane is an active dressing for the treatment of chronic wounds such as venous stasis ulcers and burns.

Objectives. Determination of the transport and internal energy conversion properties of the Textus Bioactiv Ag membrane using the Kedem–Katchalsky–Peusner model. This model introduces the coefficients L_{ij} necessary to calculate the degree of coupling (I_{ij}, Q_L), energy conversion efficiency (e_{ij}), dissipated energy (S-energy), free energy (F-energy), and internal energy (U-energy).

Materials and methods. The research material was the Textus Bioactiv Ag membrane that is used as an active dressing in the treatment of difficult-to-heal wounds, and KCl aqueous solutions. The research methods employed Peusner's formalism of network thermodynamics and Kedem and Katchalsky's thermodynamics of membrane processes. To calculate the L_{ij} coefficients, we used hydraulic conductivity (L_p), diffusion conductivity (ω) and reflection (σ) coefficients to perform experimental measurements in different conditions.

Results. The L_p coefficient for the Textus Bioactiv Ag membrane is nonlinearly dependent on the average concentrations of the solutions. In turn, the ω and σ coefficients are nonlinearly dependent on the differences in osmotic pressures (Δπ). An increase in the Δπ causes the Textus Bioactiv Ag membrane to become more permeable and less selective for KCl solutions. The coefficients of Peusner (L_{ij}), couplings (I_{ij}, Q_L), energy conversion efficiency (e_{ij}), S-energy, F-energy, and U-energy also depend nonlinearly on Δπ. Our results showed that for higher concentrations of KCl solutions transported through the Textus Bioactiv Ag membrane, the coupling and energy conversion coefficients were greater for larger Δπ up to their maximum values for large Δπ. Coupling of the membrane structure with the electrolyte flux through the membrane is observed for Δπ greater than 10 kPa.

Conclusions. Textus Bioactiv Ag membrane dressings possess the properties of a solution component separator as well as an internal energy converter.

Key words: membrane transport, polymeric membrane, energy conversion, Kedem–Katchalsky–Peusner equations, Textus Bioactiv Ag

Streszczenie

Wprowadzenie. Membrana Textus Bioactive Ag to aktywny opatrunek do leczenia ran przewlekłych, takich jak owrzodzenia żylne podudzi i oparzenia.

Cel pracy. Wyznaczenie właściwości transportowych i wewnętrznej konwersji energii w membranie Textus Bioactiv Ag, w oparciu o model Kedem–Katchalskiego–Peusnera (KKP). Model ten wprowadza współczynniki L_{ij} niezbędne do obliczenia stopnia sprzężenia (I_{ij}, Q_L), sprawności konwersji energii (e_{ij}), energii rozproszonej (S-energia), energii swobodnej (F-energia) i energii wewnętrznej (U-energia).

Materiały i metody. Badanym materiałem była membrana Textus Bioactive Ag, stosowana jako aktywny opatrunek w terapii trudno gojących się ran, oraz wodne roztwory KCl. Metody badawcze to formalizm sieciowej termodynamiki Peusnera oraz termodynamika procesów membranowych Kedem–Katchalsky'ego. Do obliczenia współczynników L_{ij} wykorzystaliśmy współczynniki przenikalności hydraulicznej (L_p), przenikalności dyfuzyjnej (ω) i odbicia (σ), zmierzone eksperymentalnie w różnych warunkach.

Wyniki. Współczynnik L_p dla membrany Textus Bioactiv jest nieliniowo zależny od średniego stężenia roztworów w membranie. Z kolei współczynniki ω i σ są nieliniowo zależne od różnicy ciśnień osmotycznych (Δπ). Wzrost Δπ powoduje, że membrana Textus Bioactiv staje się bardziej przepuszczalna i mniej selektywna dla roztworów KCl. Współczynniki: Peusnera (L_{ij}), sprzężeń (I_{ij}, Q_L), sprawności konwersji energii (e_{ij}) oraz S-energii, F-energii i U-energii również zależą nieliniowo od Δπ. Jak wynika z uzyskanych wyników, dla większych stężeń roztworów KCl transportowanych przez membranę Textus Bioactive współczynniki sprzęgania i konwersji energii są większe dla większych Δπ, osiągając wartości maksymalne dla dużych wartości Δπ. Sprzężenie struktury membrany ze strumieniem elektrolitu transportowanym przez membranę obserwuje się dla Δπ powyżej 10 kPa.

Wnioski. Opatrunek membranowy Textus Bioactive Ag posiada właściwości separatora składników roztworu, jak również wewnętrznego konwertera energii.

Słowa kluczowe: transport membranowy, membrana polimerowa, Textus Bioactiv Ag, równania Kedem–Katchalskiego–Peusnera, konwersja energii

Background

In recent years, due to the development of synthetic polymer technology, many types of synthetic membranes have found applications in modern medical therapy and diagnostics. These membranes act as selectively permeable barriers between biological tissues and the environment (e.g., hemodialyzers and active membrane dressings) or between an encapsulated drug and the internal environment of a living organism (controlled release), etc.[1–5] When treating difficult-to-heal wounds, such as venous stasis ulcers or severe burns, selecting a dressing that is designed to maintain a moist environment, suitable temperature and pH of the wound is important. Various types of active dressings have been used in the treatment of chronic wounds.[6] Their purpose is to protect nerve fibers from excessive stimulation during application and dressing changes, as well as protect delicate tissues from mechanical stimuli and external environmental influences to limit infections and bacterial contamination.[7] One type of these active dressings is the Textus Bioactiv Ag membrane dressing.[8,9] It is a composite/mixed polymer dressing containing thermoplastic polyethylene fibers and Ag zeolites.

According to the Kedem–Katchalsky (KK) model, the Textus Bioactiv Ag membrane has certain transport properties measured with the coefficients of hydraulic conductivity (of the solvent), reflection and diffusive conductivity (of the solution).[9] This means that the Textus Bioactiv Ag membrane can separate appropriate solutions of different concentrations and has the property of free energy conversion, similarly to Nephrophan or Bioprocess membranes.[10,11] The total energy of a thermodynamic system is the sum of its internal energy (nuclear, chemical and thermal) and external energy (connected with gravitational, electromagnetic, electrical field, etc.).[12]

In both biological and physicochemical membrane systems, internal energy (U-energy) is mainly chemical energy. The internal energy consists of free energy (F-energy) and degraded energy (S-energy). The F-energy, also called exergy, defines the "quality of energy" and the part of the energy that can be practically used to do work. The S-energy, also called anergy, is the passive part of the energy that cannot be used practically.[13] The conversion of chemical energy occurs in 2 stages. In the 1st stage, the F-energy is separated from the S-energy. In the 2nd stage, the F-energy is converted into useful work.

The biological cell, which functions like a chemodynamic machine, is the most efficient converter of chemical energy (U-energy) into useful energy (F-energy). The most important activity of this process is converting the F-energy contained within the chemical bonds of nutrients into high-energy compounds such as adenosine triphosphate (ATP).[14] At the expense of ATP, mechanical work, osmotic work, electrical work, and biosynthesis work are performed. The production of S-energy depends on the rate of the biochemical process: the slower the process, the greater the efficiency of the cell.[15]

Transport processes, including membrane transport, constitute a group of fundamental phenomena occurring at all levels of physicochemical systems.[16] The driving forces of these transporters are the physical quantities of scalar, vector and/or tensor nature, which participate in the creation of various types of physical fields that shape the field properties of nature. An example of a scalar field

is the field of concentrations, a vector field is the gravitational field, and a tensor field is the field of internal stresses. For a scalar field to formally participate in the creation of a thermodynamic force that generates thermodynamic flows, the appropriate gradients of scalar quantities such as concentration or temperature must be created. The generation of force results in the performance of work from the energy stored in the system.

Mathematical models developed using the framework of Onsager's linear nonequilibrium thermodynamics (LNET) and Peusner's network thermodynamics (NT)[13,17–20] are convenient tools to study membrane transport properties. One of the more important ones is the Kedem–Katchalsky–Peusner (KKP) model,[21–24] which is an extension of the KK model.[25] The classical KK equations contained transport coefficients that characterized the permeation of solvents and solutes through a membrane.[18,25] These coefficients included hydraulic permeability (L_p), reflection (σ) and solute permeability (ω). Peusner introduced L, R, H, and P versions of the KKP equations containing Peusner coefficients L_{ij}, R_{ij}, H_{ij}, and P_{ij} ($i, j \in \{1,2, \ldots, n\}$) into the science of membranes and membrane techniques.[20] The Peusner coefficients are a combination of L_p, σ and ω coefficients and the average concentration of solutions in the membrane ($\overline{C}$). The coefficients of coupling (l_{ij}, r_{ij}, h_{ij}, p_{ij} ($i \neq j$)) and energy conversion efficiency ($(e_{ij})_l$, $(e_{ij})_r$, $(e_{ij})_r$, $(e_{ij})_p$ ($i \neq j$)) can be calculated using the L_{ij}, R_{ij}, H_{ij}, or P_{ij} coefficients, respectively. In addition, the so-called coupling coefficient "Super Q", which is also a coupling measurement, can also be calculated.

In this study, the L model of the KKP form was used to evaluate the transport properties of the Textus Bioactiv Ag membrane dressing. The relationships $L_p = f(\overline{C})$, $\sigma = f(\Delta\pi)$ and $\omega = f(\Delta\pi)$ for KCl aqueous solutions were determined experimentally according to the procedures described in previous papers.[9,18] The dependencies of Peusner (L_{11}, L_{12}, L_{21}, L_{22}), coupling (l_{12}, l_{21}, Q_L) and energy conversion efficiency ($(e_{12})_l$, $(e_{21})_l$) coefficients on osmotic pressure differences ($\Delta\pi$) were calculated experimentally from the measured characteristics of L_p, σ and ω as functions of osmotic pressure. Besides, dependencies $(\Phi_S)_L = f(\Delta\pi)$, $(\Phi_F)_L = f(\Delta\pi)$ and $(\Phi_U)_L = f(\Delta\pi)$ were calculated. The $(\Phi_S)_L$ is the dissipated energy flux (S-energy), $(\Phi_F)_L$ is the free energy flux (F-energy) and $(\Phi_U)_L$ is the internal energy flux (U-energy).

Materials and methods

Membrane system

Images of the membranous Textus Bioactiv Ag (Biocell Gesellschaft fur Biotechnologie GmbH, Engelskirchen, Germany) dressing, obtained using a scanning electron microscope (SEM; Zeiss Supra 35; Carl Zeiss AG, Jena, Germany) are shown in Fig. 1A,B. These images reveal 2 types of fibers and the mesh that prevents the membrane dressing from adhering to the wound.

Textus Bioactiv Ag is a double-layer membrane dressing used to treat wounds of various etiologies.[9] It is made of 3 types of heterogeneous thermoplastic polymer fibers. The 1st layer contains polyethylene fibers, the core of which is hydrophobic and zeolites with silver ions are located on the hydrophilic surfaces. The task of the zeolites is to keep inactivated Ag^+ and/or micronized Ag inside a negatively charged polymer cage. This layer also contains hydrophilic polyethylene Super Absorbing Polymers (SAP) absorption fibers. The task of Ag^+ ions and Ag particles is to provide permanent and effective bactericidal protection of treated wounds against secondary infections. The 3rd type of polymer fibers is made of polyethylene and arranged paralelly to the skin surface, as in the 2nd layer

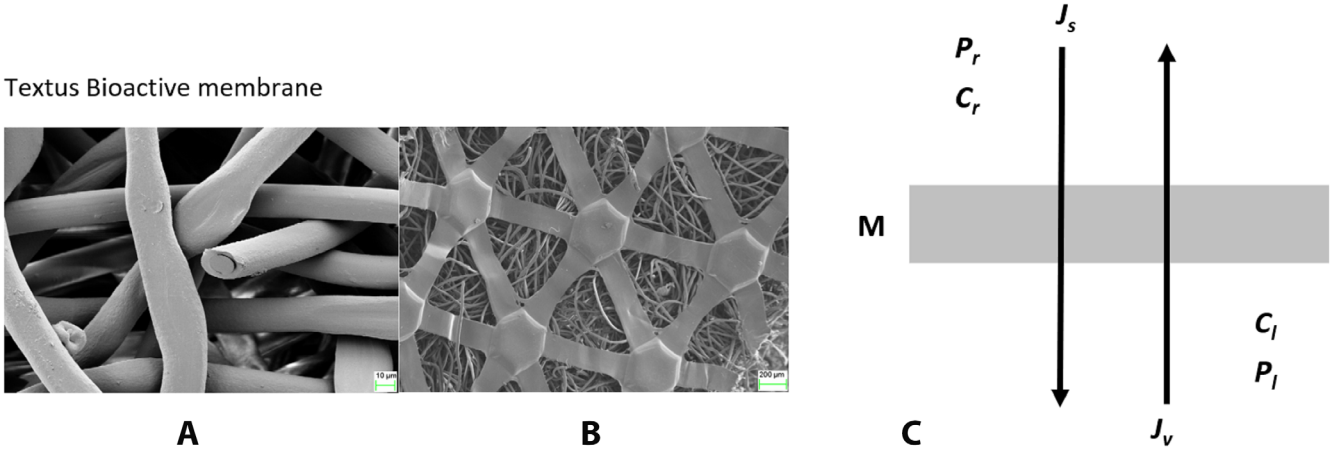

Fig. 1. Images of membrane surfaces obtained using a scanning electron microscope (SEM). A. The surface of the Textus Bioactiv Ag membrane from the side of the polymer fibers (×1740 magnification). The cross section of the fibers is visible, whose core is hydrophobic and on the hydrophilic surface of the fibers zeolites with silver ions next to the SAP fiber are visible; B. The surface of the Textus Bioactiv Ag membrane from the mesh side (×94 magnification) with polymer fibers visible in the meshes of the net; C. The single-membrane system

M – membrane; J_v – volume flux; J_s – solute flux; C_r and C_l – concentrations of solute separated by membrane; P_r and P_l – hydrostatic pressures.

of the membrane these create a special mesh that prevents the dressing from sticking to the wound. The polymer fibers used in this type of membrane are thermoplastic and able to attach to structures (zeolites, AgION™) containing silver ions. Depending on the manufacturer, membrane dressings are made of various types of fibers (polyethylene, polyamide, polypropylene, polyester, polystyrene, etc.). For example, in the case of the Textus Bioactiv Ag dressing, there are various types of polyethylene fibers, in Atrauman Ag dressing– polyamide fibers, and as in the Aquacel Ag dressing – sodium carboxymethyl cellulose fibers. The type of fibers used is important for determining the properties of the dressing. They absorb exudate and increase its volume, and prevent it from sticking to the wound (polyethylene). They ensure the correct pH (polyethylene, polyamide) or, as in the case of carboxymethyl cellulose, turn into a gel when absorbing exudate. The mesh showed in Fig. 1B has the characteristics of a non-selective membrane ($\sigma = 0$). The activation process of the dressing begins after wetting the dressing with Ringer's solution, which contains Na^+, K^+, Ca^{2+}, and Cl^- ions in various concentrations, and occurs abruptly from zeolites to SAP fibers. Due to the absorption properties of SAP fibers, the dressing has a very high absorption capability (4.2 kg/m^2).

It should be mentioned that the surface area available to the solution on the grid side (Fig. 1B) is 60.7% smaller compared to the opposite side of the membrane (Fig. 1A). If we denote the actual membrane surface area by A_h and the membrane surface area on the grid side by A_l, then $A_l \approx 0.61\ A_h$. Suppose that the A_h is in contact with a solution of concentration C_h, and the A_l is in contact with a solution of concentration C_l, then we will denote the volume flux induced by $\Delta\pi$ by J_{vh}. In this case, $\Delta\pi$ will increase solution volume (ΔV_h). If we reverse the location of the membrane, we will denote the flux for the same $\Delta\pi$, through the A_l by J_{vl}. In this case, $\Delta\pi$ will result in a solution volume increase of $\Delta V_l = 0.61\ \Delta V_h$. Given this, $J_{vh} = (\Delta V_h)A_h^{-1}(\Delta t)^{-1}$ and $J_{vl} = (0.61\Delta V_h)(0.61A_h)^{-1}(\Delta t)^{-1}$. This means that $J_{vh} = J_{vl} = J_v$. This last relationship follows the flux continuity law. Similarly, it can be shown that for the solute flux, $J_{sh} = J_{sl} = J_s$.

Mathematical model

Figure 1C shows a model of the membrane system in which the membrane (M) separates 2 homogeneous electrolyte solutions with C_r and C_l concentrations ($C_r \geq C_l$) with hydrostatic pressures of P_r and P_l ($P_r > P_l$, $P_r = P_l$ or $P_r < P_l$). For binary electrolyte solutions, the KK equations are as follows[18,26] (Equation 1–3):

$$J_v = L_p\left[\Delta P - \gamma\sigma RT(C_h - C_l) + \frac{P_E}{\kappa} I_m\right] \tag{1}$$

$$J_s = \gamma\omega RT(C_h - C_l) + \bar{C}(1-\rho)J_v + \frac{\tau_j}{z_j \nu_j F} I_m \tag{2}$$

$$I_m = -P_E J_v + \frac{\tau_j \kappa}{z_j \nu_j F}\Delta\mu_m + \kappa E \tag{3}$$

where J_v – volume flux; J_s – solute flux; I_m – electric ion current; L_p, σ, P_E and ω – coefficients of hydraulic permeability, reflection, electroosmotic permeability, and solute permeability, respectively; $\Delta P = P_r - P_l$ – difference of hydrostatic pressure; γ – Van 't Hoff coefficient; $\Delta\pi = RT(C_r - C_l)$ – differences in osmotic pressures (RT – the product of the gas constant and the absolute temperature; $\Delta\pi = RT(C_r - C_l)$ are solution concentrations, $C_h > C_l$); γ – Van 't Hoff coefficient ($1 \leq \gamma \leq 2$); κ – electrical conductivity; τ_j, z_j, ν_j – transfer number, valence and ion number, respectively; and $\bar{C} = (C_h - C_l)(\ln C_h C_l^{-1})^{-1} \approx 0.5(C_h + C_l)$ – average concentration of the solution.

If we assume that $I_m = 0$ in the system, we obtain equations analogous to those for non-electrolyte transport (Equation 4,5):

$$J_v = L_p\Delta P - L_p\gamma\sigma\Delta\pi \tag{4}$$

$$J_s = \gamma\omega\Delta\pi + \bar{C}(1-\sigma)J_v \tag{5}$$

Therefore, the membrane transport properties are characterized by the hydraulic permeability (L_p), reflection (σ) and solute permeability (ω) coefficients, the definitions of which can be presented as $L_p = (J_v/\Delta P)_{\Delta\pi=0}$, $\sigma = (\Delta P/\gamma\Delta\pi)_{Jv=0}$ and $\omega = (J_s/\gamma\Delta\pi)_{Jv=0}$.

Relatively simple algebraic transformations allow for Equation 4,5 to be written in the form (Equation 6,7):

$$J_v = L_p(\Delta P - \gamma\Delta\pi) + \bar{C}(1-\sigma)\gamma L_p\frac{\Delta\pi}{\bar{C}} \tag{6}$$

$$J_s = \bar{C}(1-\sigma)L_p(\Delta P - \gamma\Delta\pi) + \\ + \bar{C}\left[\gamma\omega + \bar{C}(1-\sigma)^2\gamma L_p\right]\frac{\Delta\pi}{\bar{C}} \tag{7}$$

The above equations are called transformed KK equations or the L version of the KKP equations.[20,22] Equation 6,7 written in matrix form containing Peusner coefficients L_{ij} ($i, j \in \{1, 2\}$) take the form of (Equation 8,9):

$$\begin{bmatrix} J_v \\ J_s \end{bmatrix} = [L]\begin{bmatrix} \Delta P - \gamma\Delta\pi \\ \gamma\dfrac{\Delta\pi}{\bar{C}} \end{bmatrix} \tag{8}$$

$$[L] = \begin{bmatrix} (L_{11})_T & (L_{12})_T \\ (L_{21})_T & (L_{22})_T \end{bmatrix} = \\ = \begin{bmatrix} L_p & L_p(1-\sigma)\bar{C} \\ L_p(1-\sigma)\bar{C} & \omega\bar{C} + L_p(1-\sigma)^2\bar{C}^2 \end{bmatrix} \tag{9}$$

Using the definition proposed by Kedem and Caplan,[20,27] the coefficients $(L_{ij})_T$ ($i, j \in \{1, 2\}$ can be used to calculate the coupling coefficients l_{12} and l_{21} defined by the expression (Equation 10):

$$l_{12} = l_{21} = \frac{L_{12}}{\sqrt{L_{11}L_{22}}} = \frac{L_{21}}{\sqrt{L_{11}L_{22}}} = \sqrt{\frac{L_p(1-\sigma)^2\bar{C}}{\omega+L_p(1-\sigma)^2\bar{C}}} \quad (10)$$

The value of the coefficients $l_{12} = l_{21} = l$ is limited by the relation that $-1 \le l \le +1$. When $l = \pm 1$, the system is fully coupled and the processes become single processes. When $l = 0$, the 2 processes are completely unconjugated and no energy conversion occurs. The definition proposed by Kedem and Caplan[27] and Peusner[20] can be used to calculate the coefficient of maximum energy conversion efficiency (Equation 11):

$$(e_{12})_L = \frac{(L_{12})^2}{L_{11}L_{22}\left(1+\sqrt{1-\frac{L_{12}L_{21}}{L_{11}L_{22}}}\right)^2} = \\ = (e_{21})_L = \frac{(L_{21})^2}{L_{11}L_{22}\left(1+\sqrt{1-\frac{L_{12}L_{21}}{L_{11}L_{22}}}\right)^2} \quad (11)$$

When Equation 10 is taken into account with Equation 11 we obtain (Equation 12):

$$(e_{21})_l = \frac{l_{21}^2}{\left(1+\sqrt{1-l_{12}l_{21}}\right)^2} = \\ = (e_{12})_l = \frac{l_{12}^2}{\left(1+\sqrt{1-l_{12}l_{21}}\right)^2} = \\ = \frac{L_p(1-\sigma)^2\bar{C}}{\left[\omega+L_p(1-\sigma)^2\bar{C}\right]\left(1+\sqrt{\frac{\omega_s}{\omega+L\ (1-\sigma)^2\bar{C}}}\right)^2} \quad (12)$$

The values of the coefficients $(e_{12})_l = (e_{21})_l = (e_{max})_l$ are limited by the relation that $0 \le (e_{max})_l \le +1$. Peusner proposed a Q_L coupling parameter called "super Q_L"[20] (Equation 13):

$$Q_L = \frac{2|L_{12}L_{21}|}{4L_{11}L_{22}-2L_{12}L_{21}} = \\ = \frac{l_{12}l_{21}}{2-l_{12}l_{21}} = \frac{(1-\sigma)^2\bar{C}}{\frac{2\omega}{L_p}+(1-\sigma)^2\bar{C}} \quad (13)$$

The coefficient Q_L is connected with $(e_{12})_l$ coefficient by using the Equation 14[15]:

$$(e_{12})_l = \frac{L_{21}Q_L}{L_{12}(1+\sqrt{1+Q_L^2})} = \\ = (e_{21})_l = \frac{L_{12}Q_L}{L_{21}(1+\sqrt{1+Q_L^2})} \quad (14)$$

According to the first law of thermodynamics, in a membrane system, when the membrane separates 2 solutions of different concentrations and the transport processes have an isothermal-isochoric character, the following equation is fulfilled (Equation 15):

$$(\Phi_U)_L = (\Phi_F)_L + (\Phi_S)_L \quad (15)$$

where $(\Phi_U)_L = A^{-1}\,dU/dt$ – flux of internal energy (U-energy); $(\Phi_F)_L = A^{-1}dF/dt$ – flux of free energy (F-energy); $(\Phi_S)_L = TA^{-1}\,d_iS/dt$ – flux of dissipation energy (S-energy); d_iS/dt is the rate at which entropy is created in the membrane system by irreversible processes (accumulated entropy flow); and T – absolute temperature. Equation 16 describes the conversions of U-energy to F-energy (exergy) and S-energy (anergy).

For one-membrane systems, $(\Phi_S)_L$ can be written in the following form (Equation 16):

$$(\Phi_S)_L = (L_{11})_T(\Delta P - \gamma\Delta\pi)^2 + [(L_{12})_T + \\ + (L_{21})_T](\Delta P - \gamma\Delta\pi)\frac{\gamma\Delta\pi}{\bar{C}} + (L_{22})_T\left(\frac{\gamma\Delta\pi}{\bar{C}}\right)^2 \quad (16)$$

Transforming the expression (Equation 17):

$$(e_{max})_L = \frac{(\Phi_F)_L}{(\Phi_F)_L + (\Phi_S)_L} \quad (17)$$

and using Equation 16 we get (Equation 18,19):

$$(\Phi_F)_L = \frac{(e_{max})_L}{1-(e_{max})_L}(\Phi_S)_L \quad (18)$$

$$(\Phi_U)_L = \frac{1}{1-(e_{max})_L}(\Phi_S)_L \quad (19)$$

Methodology for measuring the volume and solute fluxes and transport parameters

The studies on osmotic volume (J_v) and solute fluxes (J_s) were carried out using the measuring set described in a previous paper and presented in Fig. 2.[28] It consisted of 2 cylindrical vessels (l and h) with each containing a volume of 200 cm^3 of aqueous KCl solution, one with a concentration in the range of 1÷16 mol/m^3 and the other with a constant concentration of 1 mol/m^3. The solutions in the vessels were separated using a Textus Bioactiv Ag membrane dressing with an area of A = 1.15 cm^2, located in the horizontal plane.

A pipette graduated every 1 mm^3 (KP) positioned in a plane parallel to the plane of the membrane was connected to the vessel (h) containing KCl at concentration C_h. The pipette was used to measure the change in volume (ΔV) of the solution in the measuring chamber (h). The vessel (l) was connected to a reservoir containing an aqueous solution of KCl with a concentration of C_l = 1 mol/m^3, adjustable in height relative to the pipette. The measurement procedure for J_v and J_s was previously described.[18,29] Briefly, increases in the ΔV were measured under conditions of intensive mechanical stirring of the solutions

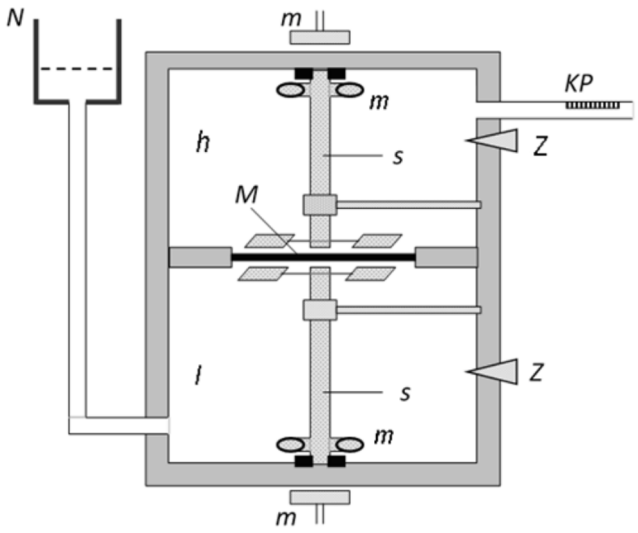

Fig. 2. Measuring system

h, l – measuring vessels; N – external solution tank; s – mechanical stirrers; M – membrane; K – calibrated pipette; m – magnets; z – plugs.[28]

at 500 rpm. The volume flux was directed from the vessel with the lower concentration to the vessel with the higher concentration of solutions, and the flow of dissolved substances was in the opposite direction. The measurements were carried out at isothermal conditions (T = 295 K).

The volume flux through the surface (A) of the membrane was calculated based on the volume changes (ΔV) over time (ΔV) measured in the pipette using the formula $J_v = (\Delta V)A^{-1}(\Delta t)^{-1}$. The fluxes of dissolved substances were calculated based on the formula $J_s = (V_u \cdot dC)A^{-1}(\Delta t)^{-1}$, where V_u was the volume of the measuring vessel and dC was the change in concentration of the solution measured with electrochemical methods.[30] The relative error in determining J_v and J_s was less than 10%. The values of coefficients coefficients L_{pT}, σ_T, and ω_T were calculated based on the formulas $L_{pT} = (J_v/\Delta P)_{Ch = Cl}$, $\sigma_T = (\Delta P/\Delta\pi)_{Jv = 0}$, and $\omega_T = (J_s/\Delta\pi)_{Jv = 0}$. Based on the characteristics $L_{pT} = f(\overline{C})$, $\sigma_T = f(\Delta\pi)$ and $\omega_T = f(\Delta\pi)$ presented in Fig. 3–5, the dependencies $L_{ij} = (\Phi_S)_L$, $L_{det} = (\Phi_F)_L$, $l_{ij} = (\Phi_U)_L$, $Q_L = f(\Delta\pi)$, $(e_{ij})_l = f(\Delta\pi)$, $(\Phi_S)_R = f(\Delta\pi)$, $(\Phi_F)_R = f(\Delta\pi)$, and $(\Phi_U)_R = f(\Delta\pi)$ were calculated.

Results

Determination of membrane transport parameters

Figures 3–5 show the dependencies $L_{pT} = f(\overline{C})$, $\omega_T = f(\Delta\pi)$ and $\sigma_T = f(\Delta\pi)$ were suitable. In the case of the $L_{pT} = f(\overline{C})$ characteristic, it was assumed that $\overline{C} \approx 0.5(C_r + C_l)$ ($C_r = C_l$). The characteristics shown in these figures are nonlinear. From the characteristics presented in Fig. 3, it follows that L_{pT} increases from $L_{pT} = 5 \times 10^{-8}$ m^3/Ns (for $\overline{C}$ = 0, pure water) to $L_{pT} = 68.5 \times 10^{-8}$ m^3/Ns ($\overline{C}$ = 8 mol/m^3)

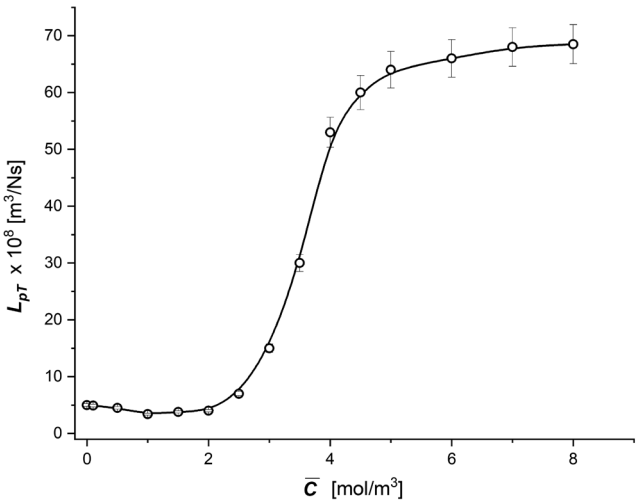

Fig. 3. Illustration of dependence $L_{pT} = f(\overline{C})$ for aqueous KCl solutions

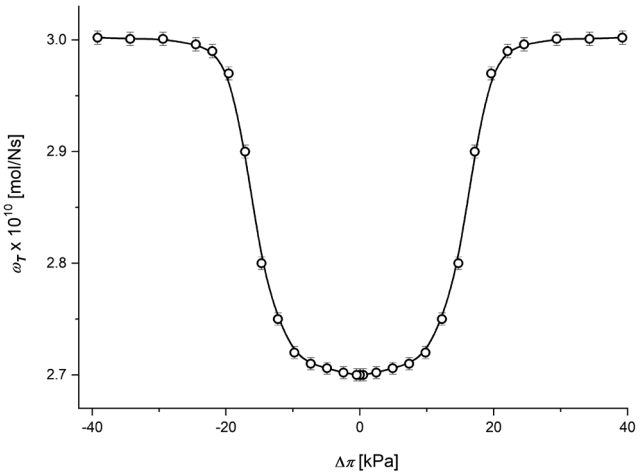

Fig. 4. Illustration of dependence $\omega_T = f(\Delta\pi)$ for aqueous KCl solutions

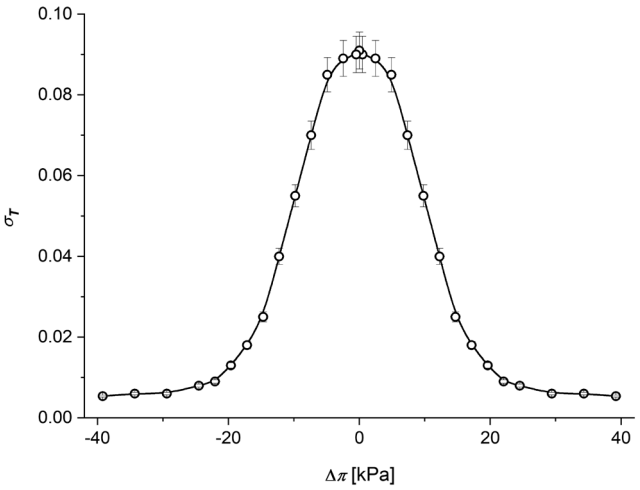

Fig. 5. Illustration of dependence $\sigma_T = f(\Delta\pi)$ for aqueous KCl solutions

– which is more than a 13-fold increase when concentrations of $\overline{C}$ changes from 0 mol/m^3 to 8 mol/m^3).

The hydraulic permeability coefficient for most membranes is constant over a wide range of membrane concentrations. As can be seen in Fig. 3, this coefficient for the Textus Bioactiv

Ag membrane is not constant. The coefficient strongly depends on the KCl concentration in the membrane with increasing concentrations in the membrane, especially for concentrations above 3 mol/m^3 (in the range of 3–6 mol/m^3). Above 6 mol/m^3, this coefficient does not change significantly. This causes a problem with the free use of the KK formalism over a wide range of electrolyte concentrations for this membrane. The relationship $L_{pT} = f(\overline{C})$ clearly shows 3 concentration ranges: an almost constant hydraulic permeability coefficient (ranges of low and high concentrations of KCl) and a transitional range of concentrations with a strong dependence of the L_{pT} coefficient on the concentration in the membrane. This indicates the complex nature of the interaction of the Textus Bioactiv Ag membrane with electrolyte solutions (aqueous KCl solutions). The strong dependence of the hydraulic permeability coefficient on the range of concentrations in the membrane may indicate possible dynamic structural changes in the membrane itself due to the interaction of its structure with electrolyte ions within the solution being transported through the membrane.

The value of coefficient ω_T increases from 2.7×10^{-10} mol/Ns (for $\Delta\pi = \pm 0.86$ kPa) to 3.0×10^{-10} mol/Ns (for $\Delta\pi = \pm 39.22$ kPa), which is an 11% increase when the concentration of $\Delta\pi$ changes from ±0.86 kPa to ±39.22 kPa (Fig. 4). Using the dependencies $\Delta\pi = \overline{C}RT\ln(C_r/C_l)$, it can be shown that $\Delta\pi = \pm 0.86$ kPa corresponds to $\overline{C} = 0.1$ mol/m^3, while $\Delta\pi = \pm 39.22$ kPa corresponds to $\overline{C} = 8$ mol/m^3. This indicates a significant change in the conditions of the solution transported through the membrane at this concentration range. This means that an increase in KCl concentrations in the Textus Bioactiv Ag membrane significantly improves the transport of KCl solutions through the membrane. Similarly to L_{pT} coefficient, the osmotic pressure ranges of almost constant value of the coefficient ω can be distinguished (low and high osmotic pressures) and the osmotic pressure range (10–20 kPa) in which increase of osmotic pressure causes an increase in the coefficient ω.

The curve in Fig. 4A shows that σ_T decreases from 0.09 (for $\Delta\pi = \pm 0.86$ kPa) to 0.005 (for $\Delta\pi = \pm 39.22$ kPa) which is related to a 18-fold reduction in the reflection coefficient when the concentration in the membrane $\Delta\pi$ changes from 0.86 kPa to 39.22 kPa. This indicates a significant reduction in membrane selectivity for KCl solutions with increasing KCl concentrations in the membrane. This nonlinear relationship of the transport coefficients is caused by swelling of the hydrophilic fibers within the membrane and by the hydration of K^+ ions. These water coatings facilitate membrane transport by reducing the friction between the membrane and the substances penetrating it, and are dependent on the concentration of the solutions. For this reason, they increase the value of L_{pT} and ω_T and decrease the value of σ_T.

The Peusner coefficients $(L_{ij})_T$

The values L_{11}, $L_{12} = L_{21}$ and L_{22} were calculated using Equation 9,10. Figures 6A–C show the nonlinear dependencies of $(L_{ij})_T = f(\Delta\pi)$ for the Textus Bioactiv Ag membrane when (a) i = j = 1, (b) i = j = 2, and (c) i ≠ j.

The value of $(L_{12})_T = (L_{21})_T$ increases from 0.04×10^{-7} m^3/Ns (for $\Delta\pi = \pm 0.86$ kPa) to 54.5×10^{-7} m^3/Ns (for $\Delta\pi = \pm 39.22$ kPa). The dependence of $(L_{22})_T = f(\Delta\pi)$ for the Textus Bioactiv Ag membrane is nonlinear and the value of $(L_{22})_T$ increases from 0.04×10^{-6} mol^2/m^{3}Ns

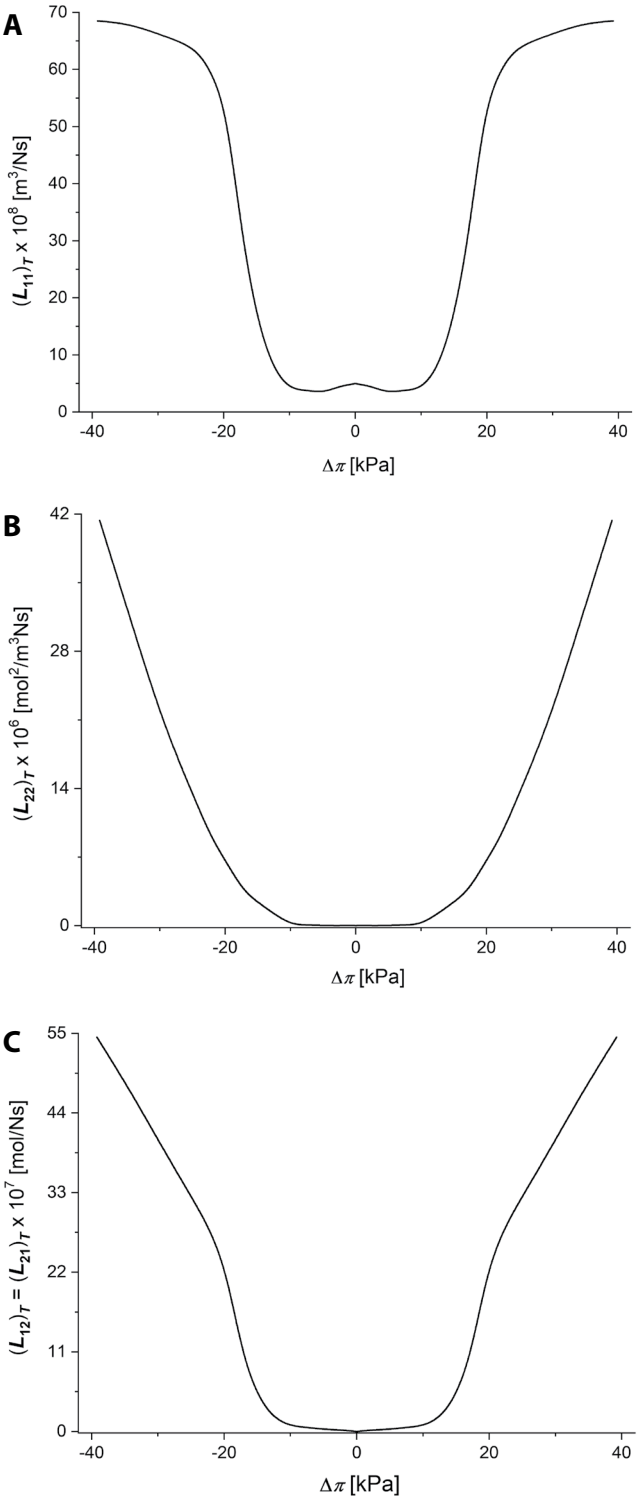

Fig. 6. Illustration of dependencies (A) $(L_{ij})_T = f(\Delta\pi)$ for i = j = 1, (B) i = j = 2, and (C) i ≠ j for Textus Bioactiv Ag membrane and aqueous KCl solutions

(for $\Delta\pi$ = ±0.86 kPa) to 41.4 × 10^{-6} mol^2/m^3Ns (for $\Delta\pi$ = ±39.22 kPa). For the $(L_{ij})_T$ coefficients for the Textus Bioactiv Ag membrane, 2 ranges of $\Delta\pi$ can be determined. For $\Delta\pi$ smaller than 10 kPa, the $(L_{ij})_T$ coefficients do not change much and are close to 0. Above $\Delta\pi$ = 10 kPa, increasing the osmotic pressure causes a gradual increase in the $(L_{ij})_T$ coefficients.

The coefficients l_{ij}, $(e_{max})_l$, and Q_L and fluxes $(\Phi_S)_L$ and $(\Phi_U)_L$

The dependencies $l_{12} = f(\Delta\pi)$, $(e_{max})_l = f(\Delta\pi)$ and $Q_L = f(\Delta\pi)$ for Textus Bioactiv Ag membranes were calculated based on Equation 11–13 and are presented in Fig. 7. As seen in Fig. 7, as the value of $|\Delta\pi|$ increases, the l_{12} coefficient for Textus Bioactiv Ag membrane fulfills the condition $l_{12} \to 1$ when $|\Delta\pi| \to 40$ kPa. In turn, as the value of $|\Delta\pi|$ increases, the value of Q_L also increases and fulfills the conditions for Textus Bioactiv Ag membrane $Q_L \to 1$ when $|\Delta\pi| \to 40$ kPa. This means that the solvent and solute transport processes are coupled to different degrees. Therefore, they act as energy converters. The measurement of energy conversion efficiency is performed using the coefficients $(e_{max})_l$ and Q_L. The curve (3) in Fig. 7 shows that the dependence $(e_{max})_l = f(\Delta\pi)$ has an identical maximum and minimum. For $\Delta\pi$ = –7.9 kPa or +7.9 kPa, the coefficient $[(e_{max})_l]_{max}$ = 0.83 and for $\Delta\pi$ = –15.35 kPa or +15.35 kPa the coefficient $[(e_{max})_l]_{min}$ = 0.53, respectively. For $\Delta\pi$ > 15.35 kPa and $\Delta\pi$ < –15.35 kPa, the dependence $(e_{max})_l = f(\Delta\pi)$ is of the saturation type. When $\Delta\pi \to -40$ kPa or +40 kPa, $(e_{max})_l \to 0.7$. As can be seen from Fig. 7, for low KCl osmotic pressures, the coefficient values are small and close to 0, which indicates a lack of process coupling in the Textus Bioactiv Ag membrane. Increasing the osmotic pressure $\Delta\pi$ on the membrane causes a fast increase in coupling coefficients, which may indicate the increasing mutual influence of the membrane structure and the electrolyte flux through the membrane. This coupling, greater for the higher applied electrolyte osmotic pressure, causes the coefficients to establish at a high level for osmotic pressures $\Delta\pi$ greater than 10 kPa, which may indicate a strong coupling between membrane structure and electrolyte flux through the membrane for high KCl osmotic pressure values on the membrane.

The dependencies $(\Phi_S)_L = f(\Delta\pi)$, $(\Phi_F)_L = f(\Delta\pi)$ and $(\Phi_U)_L = f(\Delta\pi)$ calculated based on Equation 16,18,19 for the Textus Bioactiv Ag membrane are presented in Fig. 8. The calculations were performed for a fixed difference of hydrostatic pressures ΔP = 40 kPa and different $\Delta\pi$.

As for the coupling coefficients, the energy fluxes, to a small extent, depend on $\Delta\pi$ in the range of small values of osmotic pressures on the membrane ($\Delta\pi$ < 12 kPa). An increase in the osmotic pressure on the membrane above this range causes an increase in energy fluxes on the membrane. In contrast to the coupling coefficients, which remain nearly constant at the maximum level of osmotic pressures on the membrane, the energy fluxes initially increase strongly (in the range 12 kPa ≤ $\Delta\pi$ ≤ 25 kPa), but then increase slower and slower with increases in osmotic pressures on the membrane. Moreover, in the same $\Delta\pi$ intervals, the largest values are reached by $(\Phi_U)_L$ and the smallest by $(\Phi_S)_L$.

It should be emphasized that the coupling coefficients and the energy fluxes through the Textus Bioactiv Ag membrane do not depend on the direction of applied $\Delta\pi$ on the membrane. This may indicate a different reason for the dependence of these coefficients and fluxes on the osmotic pressures of electrolytes than the 2-layer structure of the membrane. Rather, the reason for these effects may be the changes in the structure of the basic layer of the membrane itself than in the supporting layer.

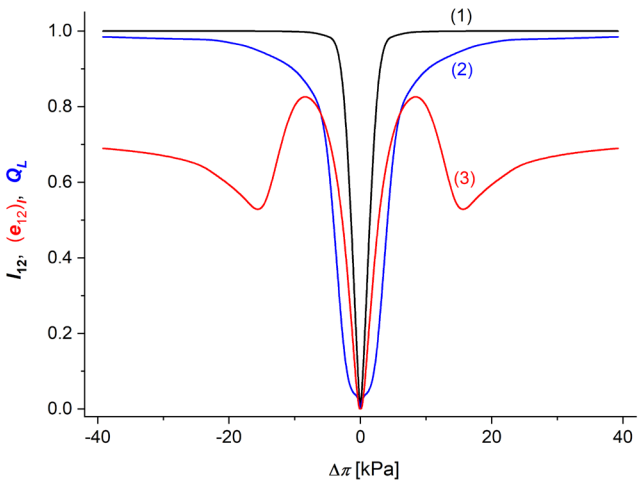

Fig. 7. Illustration of dependecies (1) $l_{12} = f(\Delta\pi)$, (2) $Q_L = f(\Delta\pi)$, and (3) $(e_{12})_l = (e_{max})_l = f(\Delta\pi)$ for Textus Bioactiv Ag membranes and aqueous KCl solutions

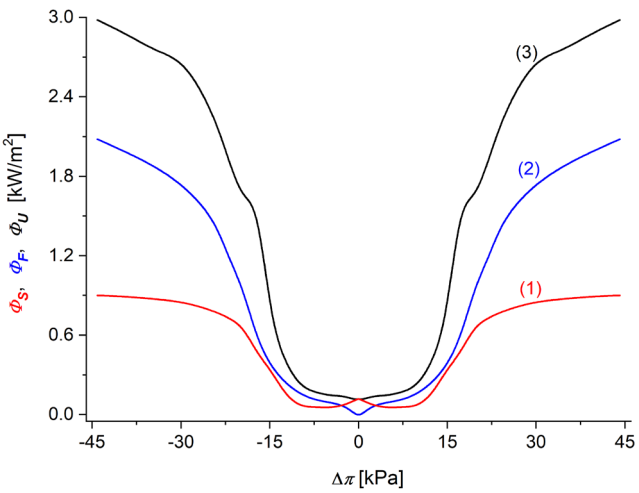

Fig. 8. Illustration of dependencies (1) $(\Phi_S)_L = f(\Delta\pi)$, (2) $(\Phi_F)_L = f(\Delta\pi)$, and (3) $(\Phi_U)_L = f(\Delta\pi)$ for Textus Bioactiv Ag membranes and aqueous KCl solutions

Discussion

The curves presented in Fig. 3–5 show that the dependencies $L_{pT} = f(\overline{C})$, $\omega_T = f(\Delta\pi)$ and $\sigma_T = f(\Delta\pi)$ are nonlinear. The L_{pT} value increases as $\overline{C}$ values increase. In turn, the value of ω_T increases with increasing values of $\Delta\pi$. Contrary to L_{pT} and ωT, the value of σ_T decreases as the value of $\Delta\pi$ increases. The courses of these curves indicate that the reason for the increase in the values of the L_{pT} and ω_T coefficients and the decrease in the value of the σ_T coefficient with increasing $\Delta\pi$ may be due to the swelling of the membrane fibers. The simultaneous increase in the volume of the membrane leads to an increase in the amount of free space for the electrolytes in the membrane. It is possible that the swelling of the fibers and the loosening of their structure in the membrane can lead to an increase in the porosity of the membrane and reduction in tortuosity of the membrane. This can be called the "relaxation" of the Textus Bioactiv Ag membrane structure under the influence of the electrolyte, and is greater for higher electrolyte concentrations in the membrane. The process of the membrane structure swelling depends on the concentration of KCl in the solutions separated by the membrane and in the membrane itself.

Contrary to the Textus Bioactiv Ag membrane, the values of the coefficients (L_p, ω, σ) of membranes made of regenerated cellulose (Nephrophan) and bacterial cellulose (Biofill) are constant (independent of the concentration of solutions separated by the membrane).[26,31] The nature of the dependence of $L_{pT} = f(\overline{C})$, $\omega_T = f(\Delta\pi)$ and $\sigma_T = f(\Delta\pi)$ is reflected in the dependencies of the coefficients $(L_{ij})_T$, as shown in Fig. 6, because these coefficients are a combination of the coefficients L_{pT}, ω_T and σ_T. In turn, the coefficients l_{12}, $(e_{max})_l$ and Q_L presented in Fig. 7 are a combination of the coefficients L_{pT}, ω_T and σ_T. Equation 16 shows that $(\Phi_S)_L$, $(\Phi_F)_L$ and $(\Phi_U)_L$ are a combination of the coefficients $(L_{11})_T$, $(L_{12})_T = (L_{21})_T$ and $(L_{22})_T$ and thus a combination of L_{pT}, ω_T and σ_T coefficients.

Conclusions

The concentration dependencies of the hydraulic permeability (L_{pT}), reflection (σ_T) and solute permeability (ω_T) coefficients for Textus Bioactiv Ag membrane are nonlinear. Significant changes of these coefficients occur in the range of KCl concentrations from 2 mol/m^3 to 4 mol/m^3. The characteristics of the Peusner coefficients $(L_{ij})_T = f(\Delta\pi)$ for the Textus Bioactiv Ag membrane are nonlinear. This characteristic feature results in the very slow increase of these coefficients with increasing osmotic pressures on the membrane in ranges lower than 10 kPa and the significantly greater increase in values above these osmotic pressures. For the Textus Bioactiv Ag membrane, the coefficients of coupling $l_{12} = l_{21}$, energy conversion efficiency $(e_{12})_l = (e_{21})_l = (e_{max})_l$, and Q_L are functions of the KCl osmotic pressure differences. This means that the processes occurring in the system containing the Textus Bioactiv Ag membrane are almost completely coupled and strong energy conversion interactions occur. For the Textus Bioactiv Ag membrane, the calculated value of free energy production $(\Phi_F)_L$ is many times higher than the value of the energy dissipation function $(\Phi_S)_L$ (e.g., for $\Delta\pi = 44$ kPa, $(\Phi_F)_L$ is over 2 times higher than $(\Phi_S)_L$). This means that the Textus Bioactiv Ag membrane has the highest energy conversion efficiency. The KKP model, by introducing additional coefficients that allow one to take into account the energetic analysis of membrane processes, is a useful tool for exploring the transport properties of biomembranes, and extends the scope of analysis of processes occurring in the membrane.

ORCID iDs

Kornelia M. Batko https://orcid.org/0000-0001-6561-3826
Izabella Ślęzak-Prochazka https://orcid.org/0000-0002-0707-2213
Sławomir Marek Grzegorczyn https://orcid.org/0000-0002-5248-3505
Anna Pilis https://orcid.org/0000-0002-5022-6820
Paweł Dolibog https://orcid.org/0000-0003-4781-5162
Andrzej Ślęzak https://orcid.org/0000-0001-6818-2099

References

1. Baker RW. *Membrane Technology and Applications*. 3rd ed. Chichester, UK-Hoboken, USA: John Wiley & Sons; 2012. ISBN:978-1-118-35971-6.
2. Giuri D, Barbalinardo M, Sotgiu G, et al. Nano-hybrid electrospun non-woven mats made of wool keratin and hydrotalcites as potential bio-active wound dressings. *Nanoscale*. 2019;11(13):6422–6430. doi:10.1039/C8NR10114K
3. Dudek-Wicher R, Paleczny J, Brożyna M, Junka A, Bartoszewicz M. Modifications of bacterial cellulose in wound care. *Polim Med*. 2021; 51(2):77–84. doi:10.17219/pim/143330
4. Shen S, Chen X, Shen Z, Chen H. Marine polysaccharides for wound dressings application: An overview. *Pharmaceutics*. 2021;13(10):1666. doi:10.3390/pharmaceutics13101666
5. Lopez-Mendez TB, Santos-Vizcaino E, Pedraz JL, Orive G, Hernandez RM. Cell microencapsulation technologies for sustained drug delivery: Latest advances in efficacy and biosafety. *J Control Release*. 2021;335:619–636. doi:10.1016/j.jconrel.2021.06.006
6. Savencu I, Iurian S, Porfire A, Bogdan C, Tomuță I. Review of advances in polymeric wound dressing films. *Reactive Functional Polym*. 2021;168:105059. doi:10.1016/j.reactfunctpolym.2021.105059
7. Kushwaha A, Goswami L, Kim BS. Nanomaterial-based therapy for wound healing. *Nanomaterials*. 2022;12(4):618. doi:10.3390/nano12040618
8. Kucharzewski M, Wilemska-Kucharzewska K, Kózka M, Spałkowska M. Leg venous ulcer healing process after application of membranous dressing with silver ions. *Phlebologie*. 2013;42(06):340–346. doi:10.12687/phleb2141-6-2013
9. Ślęzak A, Grzegorczyn S, Ślęzak IH, Bryll A. Study on the volume and solute flows through double-membranous polymeric dressing with silver ions. *J Membrane Sci*. 2006;285(1–2):68–74. doi:10.1016/j.memsci.2006.07.026
10. Batko KM, Ślęzak A, Pilis W. Evaluation of transport properties of biomembranes by means of Peusner network thermodynamics. *Acta Bioeng Biomech*. 2021;23(2):63–72. PMID:34846049.
11. Batko KM, Ślęzak-Prochazka I, Ślęzak A, Bajdur WM, Włodarczyk-Makuła M. Management of energy conversion processes in membrane systems. *Energies*. 2022;15(5):1661. doi:10.3390/en15051661
12. Boeker E, van Grondelle R. *Environmental Physics: Sustainable Energy and Climate Change*. 3rd ed. Chichester, UK: Wiley; 2011.ISBN:978-0-470-66676-0.
13. Demirel Y. *Nonequilibrium Thermodynamics: Transport and Rate Processes in Physical, Chemical and Biological Systems*. 3rd ed. Amsterdam, the Netherlands: Elsevier; 2014. ISBN:978-0-444-59581-2.

14. Glaser R. *Biophysics*. Berlin-Heidelberg, Germany: Springer Berlin-Heidelberg; 2012. doi:10.1007/978-3-642-25212-9
15. Caplan SR. Nonequilibrium thermodynamics and its application to bioenergetics. In: *Current Topics in Bioenergetics*. Vol 4. Amsterdam, the Netherlands: Elsevier; 1971:1–79. doi:10.1016/B978-0-12-152504-0.50008-3
16. Batko KM, Ślęzak A. Evaluation of the global S-entropy production in membrane transport of aqueous solutions of hydrochloric acid and ammonia. *Entropy*. 2020;22(9):1021. doi:10.3390/e22091021
17. Onsager L. Reciprocal relations in irreversible processes. *Phys Rev*. 1931;37(4):405–426. doi:10.1103/PhysRev.37.405
18. Katchalsky A. *Nonequilibrium Thermodynamics in Biophysics*. Cambridge, USA: Harvard University Press; 2013. ISBN:978-0-674-49412-1.
19. Kedem O, Katchalsky A. Permeability of composite membranes. Part 1. Electric current, volume flow and flow of solute through membranes. *Trans Faraday Soc*. 1963;59(0):1918–1930. doi:10.1039/TF9635901918
20. Peusner L. *Studies in Network Thermodynamics*. Amsterdam, the Netherlands-New York, USA: Elsevier; 1986. ISBN:978-0-444-42580-5.
21. Ślęzak A, Grzegorczyn S, Batko KM. Resistance coefficients of polymer membrane with concentration polarization. *Transp Porous Med*. 2012;95(1):151–170. doi:10.1007/s11242-012-0038-5
22. Batko KM, Slezak-Prochazka I, Grzegorczyn S, Slezak A. Membrane transport in concentration polarization conditions: Network thermodynamics model equations. *J Por Media*. 2014;17(7):573–586. doi:10.1615/JPorMedia.v17.i7.20
23. Batko KM, Ślęzak-Prochazka I, Ślęzak A. Network hybrid form of the Kedem–Katchalsky equations for non-homogenous binary non-electrolyte solutions: Evaluation of P_{ij}* Peusner's tensor coefficients. *Transp Porous Med*. 2015;106(1):1–20. doi:10.1007/s11242-014-0352-1
24. Ślęzak-Prochazka I, Batko KM, Wąsik S, Ślęzak A. H* Peusner's form of the Kedem–Katchalsky equations for non-homogenous non-electrolyte binary solutions. *Transp Porous Med*. 2016;111(2):457–477. doi:10.1007/s11242-015-0604-8
25. Kedem O, Katchalsky A. Thermodynamic analysis of the permeability of biological membranes to non-electrolytes. *Biochim Biophys Acta*. 1958;27:229–246. doi:10.1016/0006-3002(58)90330-5
26. Grzegorczyn S, Ślęzak A. Kinetics of concentration boundary layers buildup in the system consisted of microbial cellulose biomembrane and electrolyte solutions. *J Membrane Sci*. 2007;304(1–2):148–155. doi:10.1016/j.memsci.2007.07.027
27. Kedem O, Caplan SR. Degree of coupling and its relation to efficiency of energy conversion. *Trans Faraday Soc*. 1965;61:1897. doi:10.1039/tf9656101897
28. Ślęzak A, Grzegorczyn S, Jasik-Ślęzak J, Michalska-Małecka K. Natural convection as an asymmetrical factor of the transport through porous membrane. *Transp Porous Med*. 2010;84(3):685–698. doi:10.1007/s11242-010-9534-7
29. Ślęzak A. Irreversible thermodynamic model equations of the transport across a horizontally mounted membrane. *Biophys Chem*. 1989;34(2):91–102. doi:10.1016/0301-4622(89)80047-X
30. Grzegorczyn S, Michalska-Małecka K, Slezak A. Time evolution of NaCl flux through the microbial cellulose membrane with concentration polarization. *Polim Med*. 2008;38(2):11–20. PMID:18810983.
31. Ślęzak A, Jasik-Ślęzak J, Grzegorczyn S, Ślęzak-Prochazka I. Nonlinear effects in osmotic volume flows of electrolyte solutions through double-membrane system. *Transp Porous Med*. 2012;92(2):337–356. doi:10.1007/s11242-011-9906-7